Solid State Communications 149 (2009) 352–356

Contents lists available at ScienceDirect

Solid State Communications

journal homepage: www.elsevier.com/locate/ssc

Blue–violet photoluminescence from colloidal suspension of nanocrystalline silicon in silicon oxide matrix

Mallar Ray [a,*], Kakali Jana [a], N.R. Bandyopadhyay [a], S.M. Hossain [b,1], Daniel Navarro-Urrios [b], P.P. Chattyopadhyay [c], Martin A. Green [d]

[a] School of Materials Science and Engineering, Bengal Engineering and Science University, Shibpur, Howrah 711103, West Bengal, India
[b] Dipartimento di Fisica, Università di Trento, Via Sommarive 14, 38100 Povo, Italy
[c] Department of Metallurgy and Materials Engineering, Bengal Engineering and Science University, Shibpur, Howrah 711103, West Bengal, India
[d] ARC Photovoltaics Centre of Excellence, University of New South Wales, Sydney 2052, Australia

ARTICLE INFO

Article history:
Received 1 August 2008
Received in revised form
2 December 2008
Accepted 11 December 2008 by D.D. Sarma
Available online 24 December 2008

PACS:
78.55.-m
81.20.Ev
78.55.Ap
61.46.Hk

Keywords:
A. Silicon nanocrystal
B. Mechanical milling
C. Blue–violet photoluminescence

ABSTRACT

We report room temperature visible photoluminescence (PL), detectable by the unaided eye, from colloidal suspension of silicon nanocrystals (nc-Si) prepared by mechanical milling followed by chemical oxidation. The PL bands for samples prepared from Si wafer and Si powder peak at 3.11 and 2.93 eV respectively, under UV excitation, and exhibit a very fast (∼ns) PL decay. Invasive oxidation during chemical treatment reduces the size of the nc-Si domains distributed within the amorphous SiO_2 matrix. It is proposed that defects at the interface between nc-Si and amorphous SiO_2 act as the potential emission centers. The origin of blue–violet PL is discussed in relation to the oxide related surface states, non-stoichiometric suboxides, surface species and other defect related states.

1. Introduction

Since Canham's [1] report on room temperature light emission from porous Si, there has been great interest surrounding the topic aimed at understanding the origin of PL and possible application in light emitting devices. Efficient room-temperature PL has been obtained from nc-Si embedded in SiO_2 matrix, having adequate structural stability for reliable fabrication of solid light emitters [2]. A wide range of PL emission bands ranging from UV to NIR have been reported for such systems prepared by different techniques, like crystallization of amorphous SiO_2, Si^+ implantation in SiO_2, Si rich SiO_2 grown by chemical vapor deposition or by sputtering, etc. It has been demonstrated that stable luminescence of nc-Si in Si oxide films peaks in the NIR region even when the size of nc-Si is ∼2 nm [3], implying difficulties in obtaining efficient visible luminescence, especially in the blue–green range [4].

Earlier studies have examined the microstructural features induced in elemental Si by high energy ball milling [5–7]. Milling of elemental Si in Spex-8000 shaker mill in sealed argon atmosphere resulted into two phase amorphous and nc-Si [6]. Shen et al. [7] have shown room temperature PL emission with peak positions ranging from 890 to 900 nm from nc-Si in Si-oxide matrix prepared by high energy ball milling. In this communication, we report intense violet–blue emission from colloidal suspensions of nc-Si in Si-oxide matrix prepared by chemically induced oxidation of mechanically milled Si. To the best of our knowledge there has been no previous report on blue PL from nc-Si prepared by ball milling. The novel and inexpensive synthesis route of nc-Si in oxide matrix, exhibiting blue–violet PL, opens up a huge scope for potential applications.

2. Experimental details

Si powder from two different sources were used as starting materials — (i) commercial Si powder, with average particle size 20 μm, purchased from Alfa Aesar with nominal purity of 99.9% (sample: S1) and (ii) Si powder prepared from 2–5 Ω cm resistivity,

* Corresponding author. Tel.: +91 33 26688140; fax: +91 33 26682916.
E-mail address: mray@matsc.becs.ac.in (M. Ray).
[1] Permanent address: Department of Physics, Bengal Engineering and Science University, Shibpur, Howrah 711103, India.

0038-1098/$ – see front matter © 2008 Elsevier Ltd. All rights reserved.
doi:10.1016/j.ssc.2008.12.023

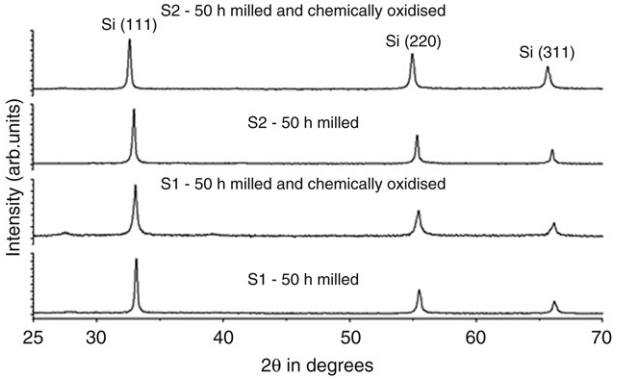

Fig. 1. XRD patterns of nc-Si prepared by 50 h of ball milling of S1 and S2 followed by chemical etching.

p-type, (100) orientation, Czochralski grown crystalline Si-wafers (sample: S2). The lightly B-doped, p-type wafers were first crushed using a silica mortar and pestle to reduce the average particle size below 1 mm. Mechanical milling of both the samples were performed in a Fritsch P6 planetary ball mill operated at 250 rpm with a ball-to-powder weight ratio of 10:1, using WC vial (250 mL) and balls (10 mm) for 50 h duration. Toluene was used as the milling medium to minimize oxidation and agglomeration. The ball milled Si powder was transferred in a clean and covered Petri dish and allowed to dry for 3 weeks in a glove box in nitrogen environment. A standard Piranha etch of the dried powder with 2:1 solution of H_2SO_4 (98%) and H_2O_2 (30%) was carried out to remove any trace organic and metallic contaminants [8]. The solution of Si powder (approximately 0.5 gm) in H_2SO_4 and H_2O_2 solution (5 mL) was then slowly heated at around 110 °C until the entire liquid evaporated and dry deposits of oxygen rich Si nanocrystals were obtained. The heating was carried out in ambient atmosphere inside a fume hood to promote sufficient oxidation. Subsequently, the particles were dissolved in isopropyl alcohol and sonicated to prepare colloidal suspension of particles made of nc-Si embedded in SiO_2. Intense visible luminescence under 365 nm UV excitation could be observed by the naked eye from the colloidal solution prepared from both the samples.

The as-milled and chemically etched powder for S1 and S2 were characterized by X-ray diffraction (Fig. 1) using a PW3710 based Phillips diffractometer with Co, $K_{\alpha 1}$ radiation (1.789 Å), and average particle size was estimated using Voigt analysis [9]. The optical absorption spectra were obtained using a Varian Cary 50 UV-Vis spectrophotometer. PL and PL excitation (PLE) measurements of the colloidal suspensions were carried out using a Horiba Jobin Yvon, FluoroMax-4 Spectrofluorometer with a Xenon source. The excitation wavelengths were chosen from the PLE measurements. Time resolved PL spectra of S1 sample under pumping with the third harmonic line of the Nd:YAG (355 nm) was recorded in 200 ns window for the wavelength range of 350–440 nm. Appreciable PL signal was obtained for energies below 380 nm for S1. Samples for HRTEM were prepared by dip coating the nc-Si on copper grids after thorough sonication of the colloidal suspensions.

3. Results and discussions

The XRD pattern shown in Fig. 1 clearly reveals the crystallinity of Si after chemical oxidation without detectable presence of any contaminant. The different planes of Si are indexed according to JCPDS card: 27-1402. The reduction in average Si crystallite sizes after oxidation step is shown in Table 1.

Optical absorption measurements were carried out for both the samples S1 and S2 in an attempt to estimate the shift in absorption

Table 1
Average particle size of the nc-Si calculated from the most significant peak of the XRD plots.

	Average crystallite sizes (in mm) for samples prepared from	
	Si powder (S1)	Si wafer (S2)
After 50 h milling	55	53
After Piranha etch	34	48

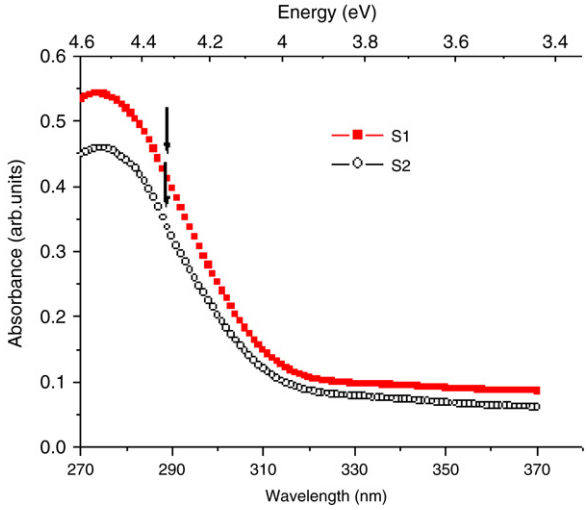

Fig. 2. UV-Vis absorption spectra of the colloidal suspensions of nc-Si, S1 and S2. The adsorption edges calculated from the point of inflection are marked with arrows and correspond to 4.3 eV for both S1 and S2.

edge of the nc-Si with regards to bulk Si. Quantitative estimation of the indirect as well as the direct band gaps were made using Tauc's method [10] and also from the point of inflection in the absorption spectrum [11]. The absorption curves for S1 and S2 are shown in Fig. 2 and the absorption edges calculated from the point of inflection are marked with arrows. The indirect optical energy gaps were calculated from Tauc's plot by extrapolating the linear portions of $(\alpha h\nu)^{1/2}$ vs. $h\nu$ plot, where $h\nu$ is the photon energy, to $(\alpha h\nu)^{1/2} = 0$. The effect of phonon scattering was taken into account by using the relation $\sqrt{\alpha h\nu} \propto (h\nu - E_g \pm E_p)$, where E_g is the optical band gap and E_p is the phonon energy involved in the indirect process. The indirect band gaps calculated in this manner, as shown in Fig. 3(a), are 2.1 and 2.5 eV for S1 and S2 respectively. Following a similar technique, the direct band gap was estimated to be 4 eV, from the intercept of the linear part of $(\alpha h\nu)^2$ vs. $h\nu$ at $(\alpha h\nu)^2 = 0$ (Fig. 3(b)).

The measured optical response of nanocrystals reflects the combined contribution of absorption and scattering. In an attempt to account for the effect of scattering, the equation $\alpha = \frac{\beta(h\nu - E_g)^{1/2}}{h\nu} + \gamma\nu^4$ was fitted to the α vs. $h\nu$ plot by treating β, E_g and γ as fitting parameters. However, the value of the band gap calculated remains the same i.e. 4 eV, even after incorporating a term accounting scattering. It should be noted here that our system comprises of a population of nc-Si particles in an oxide matrix with significant dispersion in crystallite sizes, along with obvious presence of defects introduced during ball milling and forced oxidation. Therefore, the band edge energy calculated from the absorption curves gives an average value that contains the effect of different contributing factors, typical for any polydispersed population.

The TEM micrographs of the chemically oxidized sample (Fig. 4(a) and (b)) reveal presence of both amorphous and crystalline phases with perceptible variation in crystallite size. The larger nc-Si domains are highly disordered and contain defects

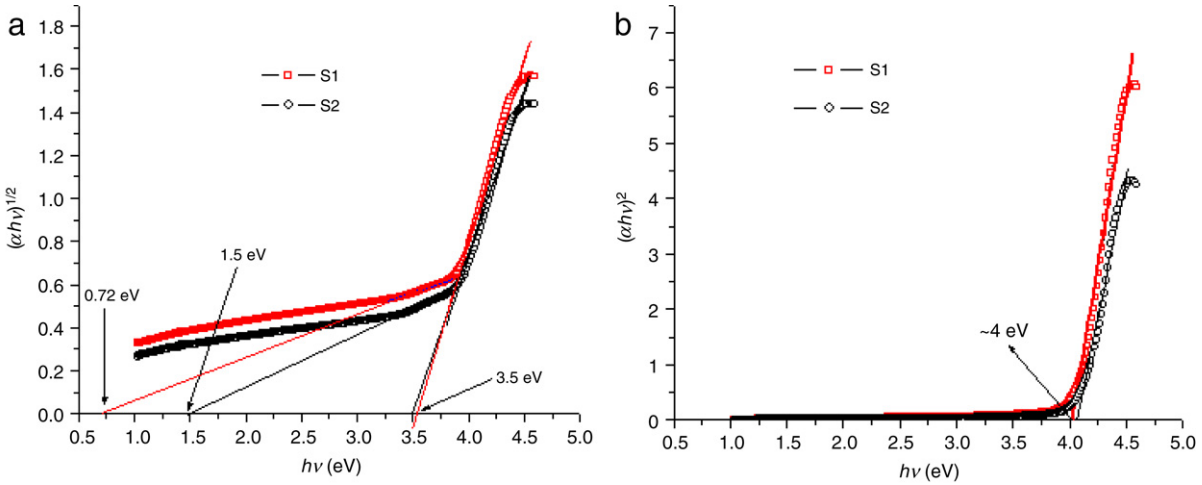

Fig. 3. Tauc plot for calculation of indirect and direct optical band edge energies. (a) $(\alpha h\nu)^{1/2}$ vs. $h\nu$ plot, where $h\nu$ is the photon energy. The intercepts for $(\alpha h\nu)^{1/2} = 0$, as indicated in the graph, correspond to $E_g + E_p$ and $E_g - E_p$, where E_g is the optical energy gap and E_p is the phonon energy required for indirect transition. (b) Plot of $(\alpha h\nu)^2$ vs. $h\nu$. The estimated direct band gap at 4 eV is marked by an arrow.

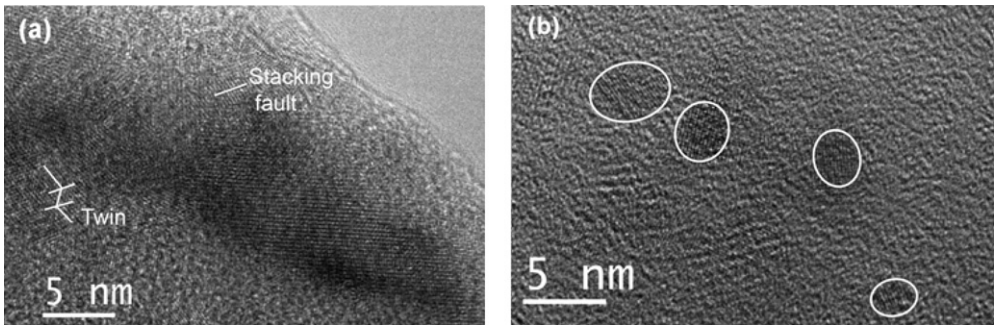

Fig. 4. HRTEM images of chemically oxidized sample (S2) (a) showing relatively large crystalline islands with manifold defects. A distinctly identifiable twin and a stacking fault are marked, and (b) showing the presence of smaller crystals. Some of the crystalline islands with diffused and ill-defined boundaries are shown.

like twins, stacking faults etc., which have earlier been reported as the microstructural features of mechanically milled nc-Si [5]. The smaller crystalline domains with sizes ∼5 nm and less, as shown in Fig. 4(b), do not contain any discernible density of defects. It is also evident that the boundaries of the crystallites are ill-defined, which is suggestive of invasive oxidation of the Si powders forming islands of nc-Si in an amorphous silicon oxide matrix.

In the present study, no perceptible visible PL signal was obtained from the ball milled S1 and S2 samples. Chemical oxidation of both the samples resulted in intense visible PL, as shown in the inset (ii) of Fig. 5(a). The excitation energies for S1 and S2 were 3.54 eV (350 nm) and 3.76 eV (330 nm) respectively, which were chosen from the PLE curves shown in the inset (i) of Fig. 5(a). The PL spectra clearly indicates violet–blue emission from both S1 and S2 with PL band peaks at 422 nm (2.93 eV) and 398 nm (3.11 eV), respectively, indicating a marginal blue shift for the sample prepared from milling of lightly B doped Si wafer compared to that prepared from Si powder.

The origin of PL in low dimensional Si structures has been debated since the discovery of light emission from porous Si and the issue still awaits a consensus. Several models have been suggested so far, which include quantum confinement of excitons [1], oxide related surface states [12], defect centers in silicon oxide and sub-oxides [13], emission from chemical species [14], etc. Blue emission from Si implanted in Si oxide layers has also been reported and attributed to non-stoichiometric composition of silicon dioxide [15,16]. In this work, the size of nc-Si islands revealed in the TEM study of the oxidized S1 and S2 samples are greater than 5 nm, except for a few (e.g., Fig. 4(b)). It is difficult to ascertain that TEM images will give truly representative particle dimensions in the absence of large statistical samples. Moreover, average particle size (Table 1) indicates a wide size distribution with negligible fraction, having dimensions ∼2 nm. Such observation allow us to exclude the 'exclusive' role of quantum confinement in the emission of visible blue luminescence shown in Fig. 5(a), as the same would require nc-Si with size ∼2 nm or less for which the band gap is ≥2.7 eV [17]. The second possibility is that blue PL arises from silicon oxide matrix. However, the excitation energy required to obtain visible luminescence from SiO_2 is much greater than 330 nm (which is the maximum excitation energy in our case), and is not enough to create non-equilibrium carriers across the band gap of SiO_2. But in the presence of non-stoichiometric suboxide of silicon, the band gap is much smaller and may produce non-equilibrium carriers under UV excitation [18]. A third possibility may be that violet–blue PL arises from oxygen related shallow surface states produced by Si–O bonds at the interface of the nc-Si and SiO_2 as proposed by Tsybeskov et al. [13] in an attempt to explain the origin of blue PL band obtained from porous silicon. These states should be shallow because of the very fast decay time (<6 ns) obtained from the time resolved PL (Fig. 5(b)) indicating extremely short carrier lifetimes. However, it is difficult to establish from the results that shallow oxygen related surface states at the interface of the nc-Si and SiO_2 are the principle contributors. It is expected that, in such a case, the PL spectrum should also have red or IR bands corresponding to other radiative transitions typical of oxidized nc-Si in SiO_2.

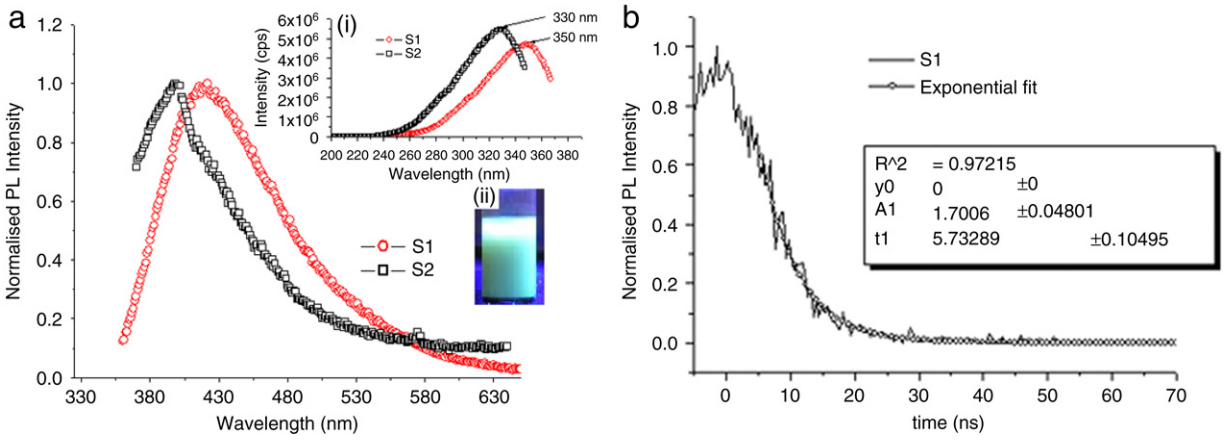

Fig. 5. Normalized PL spectra of colloidal suspension of nc-Si in Si-oxide matrix prepared by chemical oxidation of ball milled Si. (–○–) PL spectrum of S1, under 350 nm UV excitation; (– –) PL spectrum of S2 with an excitation of 330 nm. The inset (i) is the PLE spectra of S1 and S2 monitored at 400 nm, and inset (ii) shows the photograph of intense visible luminescence from the colloidal suspension of sample prepared from S2, under 365 nm UV excitation. (b) Time resolved PL spectra of S1 showing a decay time < 6 ns, from a first order exponential fit. The pump pulse width is about 6 ns, which means that the PL decay could be even faster than the value extracted from the exponential fit.

In the extensive study of colloidal Si nanoclusters synthesized in inverse micelles, Wilcoxon et al. [19] have reported PL peaks ranging from 1.8–3.6 eV for different cluster sizes and for different excitation energies. For excitation at 256 nm, their samples exhibited two PL peaks, an intense peak at 365 nm and a weaker peak at 600 nm. While the origin of the intense high energy peak was ascribed to a direct electron hole recombination at $\Gamma(\Gamma_{25}-\Gamma_{15})$, the weaker peak was tentatively assigned to phonon assisted indirect recombination. In our case, the PL peak is below the direct band gap, by about 1 eV. Thus the possibility of dominant direct recombination seems remote. Absence of red or IR bands in the PL spectrum does not support predominant phonon assisted transitions from interface states. According to the comparison of various reported data made in [19], the origin of our PL peaks could be associated with surface chromophores. This conjecture is also supported by the findings of Ding et al. [20] where they report that nc-Si have the ability to store charges in solution, which can subsequently lead to light emission upon electron and/or hole transfer. The PL peaks observed from solution of 2 nm (almost monodispersed) nc-Si capped with hydrogen and alkoxide, for 360 nm excitation, was around 400 nm, and that agrees well with our result. However, for our samples, it would be difficult to definitively assert on this origin. As discussed above, the nc-Si of the samples (S1 & S2) are polydispersed, and the possibility of the existence of substantial 2 nm particles is extremely remote. The absence of detectable PL signal from the as-milled sample with the same background solution also poses a difficulty in assigning the origin to surface related species. Thus a determining role of the background solution — isopropanol and ethanol in this case, to produce surface complexation with nc-Si so as to yield blue PL, is very unlikely. However, the possibility of introduction of surface species during Piranha etch (which was carried out to remove trace metallic and organic contaminants, if any) cannot be completely ruled out at this stage of investigation.

Finally, we explore the possibility of the defect related origin of blue–violet PL. It seems obvious that defects inside the nc-Si islands are not responsible. Absence of visible PL in the untreated ball milled sample which contains abundance of these defects (Fig. 4(a)) allows us to eliminate the role of these 'bulk' defects in emission of violet–blue PL. But it would be interesting to consider the effect of highly localized defects at the nc-Si/SiO_2 interface. A recent study by Godefroo et al. [21] based on measurements of PL in pulsed magnetic fields up to 50 T, show that defects at the interface of Si embedded in SiO_2 are the dominant source of light. We are inclined to believe that in our case, chemical treatment of the ball milled nc-Si samples enhances the specific surface area for individual nc-Si domains due to invasive oxidation. This introduces highly localized defects at the Si/SiO_2 interface which act as emission centers. In addition, a very fast decay (∼ns) is in conformation with the defect related PL emission model.

PL from paramagnetic defect centers like the well known P_b-center (≡Si^*) or non-bridging oxygen hole center (NBOHC) emit at energies that normally peak at 1.7–1.9 eV [7,22] and are hence unlikely to explain the origin the observed PL. However, the PL peaks of our system are close to the reported 2.7 eV peak observed under 5 eV excitation in Si implanted SiO_2 film [23]. This has been attributed to neutral oxygen vacancy (NOV) [24]. NOV induces very strong and anisotropic lattice distortion, and the defect formation energies are strongly dependent on the extent of lattice induced defect distortion [25]. It is possible that chemical treatment of the milled Si produces a structure that causes relaxation of the atoms surrounding the neutral vacancy. This in turn has an impact on energies of the triplet state of the diamagnetic defect center thereby accounting for blue shift of the PL bands in our system compared to the previously reported 2.7 eV peak. These are only qualitative assessments to account for the role of non-stoichiometric suboxide, surface states and defect related states in an attempt to investigate the mechanism of blue–violet PL. It is imperative to mention here that the aforesaid quantitative assessment warrants further studies.

4. Conclusion

In summary, we have synthesized a colloidal suspension of particles made of nc-Si islands in silicon oxide matrix by an inexpensive technique of ball milling Si followed by chemical oxidation. The colloidal suspension exhibited intense visible PL under UV excitation with PL band that peaks at 3.11 and 2.93 eV for samples prepared from Si wafer and Si powder, respectively. The origin of blue–violet PL at room temperature is probably due to the defect states introduced at the interfaces between nc-Si islands and amorphous SiO_2 matrix due to invasive oxidation of chemically treated ball milled nc-Si. However the role of oxygen related surface states, surface species and non-stoichiometric suboxides cannot be completely ruled out in explaining the origin of observed PL, at this stage of investigation. The finding opens up the scope for quantitative assessment for microscopic origin of such strong blue–violet PL.